Impact Tests of Flexible Nonmetallic Aircraft Fuel Tanks Installed in Two Categories of Simulated Wing Structures

by

Charles V Bennett

and

Robert J Schroers

Aircraft Division

TECHNICAL DEVELOPMENT REPORT NO. 291

CIVIL AERONAUTICS ADMINISTRATION
TECHNICAL DEVELOPMENT CENTER
INDIANAPOLIS, INDIANA

January 1957

U S DEPARTMENT OF COMMERCE
Sinclair Weeks, Secretary

CIVIL AERONAUTICS ADMINISTRATION
James T Pyle, Administrator
D M Stuart, Director, Technical Development Center

TABLE OF CONTENTS

IMPACT TESTS OF FLEXIBLE NONMETALLIC AIRCRAFT FUEL TANKS INSTALLED IN TWO CATEGORIES OF SIMULATED WING STRUCTURES*

SUMMARY

Tests have been conducted at the Technical Development Center of the Civil Aeronautics Administration to correlate the ability of a nonmetallic aircraft fuel tank to resist rupture under impact loads with material strength and/or energy-absorbing properties The nonmetallic tanks were housed in two types of simulated wing structures with chordwise strength characteristics equivalent to those of a modern twin-engine and a modern four-engine airplane

The results of the tests indicate that impact resistance of the test unit varies linearly with fuel-cell material strength and energy-absorbing properties for materials of similar basic construction The impact resistance of the test unit for fuel-cell materials of equal strength is affected greatly by the construction of the fuel cell

Protection for the nonmetallic fuel container is provided by the surrounding structure, therefore, an appreciable increase in crash resistance may be obtained by increasing the strength of the surrounding structure

INTRODUCTION

The CAA Technical Development Center, in cooperation with the United States Rubber Company and the Goodyear Tire and Rubber Company, and under joint sponsorship of the Departments of the Air Force and Navy, is engaged in a program to develop crash-resistant fuel tanks for aircraft These tanks are intended to prevent loss of fuel and thereby help to eliminate the occurrence of destructive fires during aircraft accidents and crashes of the type in which the occupants normally would be expected to survive the crash impact

The first phase of the investigation[1] involved the testing of full-scale fuel tanks under simulated crash conditions The results of this investigation indicated that nonmetallic flexible tanks, which possess sufficient strength and/or energy-absorbing properties to resist rupture while the surrounding structure begins to disintegrate, offer good possibilities for a reasonable and practical solution to the problem The second phase of the investigation[2] was undertaken to determine the strength and energy-absorbing properties of some proposed fuel-cell materials to aid in the selection of such materials for use in the fabrication of full-scale crash-resistant fuel tanks for subsequent testing under simulated crash conditions

The present investigation was conducted to establish the relationship between the ability of a nonmetallic flexible tank to resist rupture under impact loads and its tensile strength and/or energy-absorbing properties The impact resistance was determined for a number of bladder-cell materials housed in simulated aircraft-wing structures

The terms "material," "bladder-cell material," "fuel-tank material," and equivalent expressions in this report denote a composite, nonmetallic, flexible, elastomer-impregnated fabric arranged in layers or plies The terms "bladder cell," "fuel cell," and "bladder-type fuel tanks" denote a fuel container fabricated of these materials They may apply to bladder-type fuel tanks which are complete in themselves or to removable jackets or boots inside of which the cell actually containing the fuel might be encased

---

*Manuscript submitted for publication July 1956

[1] R L Field, Melvin F Miller, and George L Pigman, "An Investigation of the Crash-Fire Problems in Transport Aircraft Fuel Tanks," CAA Technical Development Report No 134, January 1951

[2] Richard N Motsinger, Melvin F Miller, and Robert J Schroers, "Some Physical Properties of a Number of Proposed Constructions of Materials for Nonmetallic Crash-Resistant Aircraft Fuel Tanks," CAA Technical Development Report No 220, December 1953

BASIC CONSIDERATIONS

Review of Accident Studies and Early Crash Tests

Studies of aircraft accidents and accident records indicate that there is no well defined standard crash condition for which crash-resistant fuel tanks can be designed. Many combinations of impact and inertia forces may be applied to wing fuel tanks and supporting structures in crashes, causing severe damage to the structures and tanks while little damage may be experienced by the fuselage or passenger compartments.[3] The impact forces on wings during crashes are principally in a rearward and upward direction, with resulting inertia forces acting in opposite directions.

From some simulated crash tests conducted subsequent to completion of the first part of the investigation,[3] it has been concluded that among the various types of loads which can be experienced by wing fuel tanks during crash conditions, the concentrated type of impact load on the leading edge or lower surface of the wing in the region of the fuel tank is the most severe, and it should be considered as the design condition for the tanks. This type of crash load was imposed on the experimental tanks by propelling them into a backstop. This test has been used exclusively for the work described in this report.

Design Criteria for Crash-Resistant Fuel Tanks

Prior to the present investigation there were no available data which could be used as a reliable guide to determine how strong a crash-resistant fuel tank should be. In an attempt to define fuel-tank crash strength in terms of accident severity, the concept has been adopted that fuel tanks should be capable of resisting rupture in the types of accidents and crashes in which the passengers normally would be expected to survive the crash impact. The criterion developed from this concept and used as a basis for establishing the magnitude of impact loads to be used in the simulated crash tests of this program is that crash-resistant fuel tanks in wings should not rupture from the effects of impact loads having sufficient magnitude to tear the wing from the aircraft. This concept is illustrated in Fig. 1. Further, it is considered that any loads applied to fuel tanks in wings need not be greater than those which would cause seat belts in the cabin to be broken. In the type of crash condition being considered, it is assumed that the aircraft is substantially under control, making an emergency landing on moderately rough terrain, and that the wing-impact loads are applied generally in a rearward and upward direction.

From an analysis of the chordwise strength characteristics of aircraft wings and from crash experience, it is known that the wings can be torn from an aircraft without imposing inertia loads on the occupants sufficiently high to break seat belts. Therefore, it appears that, except possibly for extreme inboard locations on the wing, there is no relationship between wing fuel-tank crash strength and seat-belt strength.

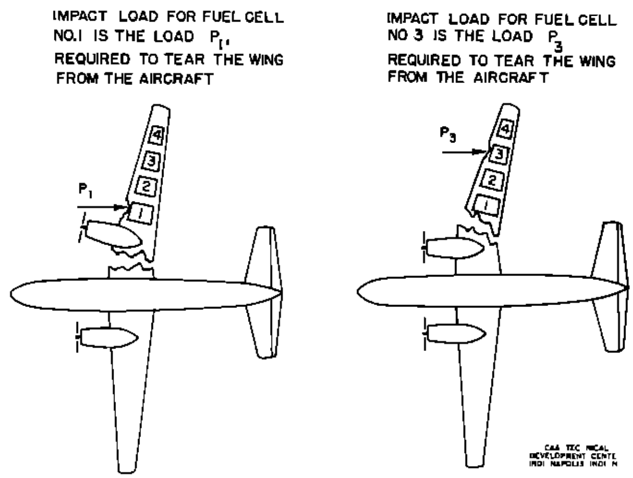

Fig. 1 Concept on Magnitude of Crash-Resistant Fuel Tanks in Wings

---

[3] Field, Miller, and Pigman, op. cit.

APPARATUS

Fifty experimental bladder cells, consisting of five groups with ten cells in each group, were constructed of materials selected on the basis of previous test results. In making these selections emphasis was placed on the strength and energy-absorbing properties of the materials. Very little consideration was given to weight. The cells in each group had strength and energy-absorbing properties different from those of the other groups. The strength and energy-absorbing properties of samples of the materials were determined from tests using a compressed-air gun.[4] A brief description of the materials used in the construction of the cells is given in Table I.

The impact tests were conducted with the bladder cells installed in simulated aircraft-wing structures having approximately equivalent strength characteristics of the wings of two categories of transport-type aircraft. Two groups of 25 structures each were built for the tests. The Type A structure possessed strength characteristics equivalent to those of the midspan station of the wing of a modern twin-engine airplane with a gross weight of 53,000 pounds. The strength characteristics of the Type B structure represented those of the one-third-span station of a modern four-engine airplane with a gross weight of 147,000 pounds. Both types of structures were provided with a compartment for the experimental fuel cells of 180-gallon capacity. Pertinent dimensional characteristics of the simulated wing structures are shown in Fig. 2. A view of a Type B structure is shown in Fig. 3. The Type A structure is similar in appearance.

TABLE I

DESCRIPTION OF FUEL-CELL MATERIALS AND DIAPHRAGM BURST-TEST RESULTS

Fuel-Cell Material No.	Description	Tensile Strength* (pound per inch width)	Energy-Absorption* (inch pounds)	Elongation* (per cent)
1	Two-ply, lightweight, plain weave, nylon fabric, Buna-N coated.	240	33,300	28.5
2	Two-ply, heavy weight, plain weave, nylon fabric, Buna-N coated	840	141,600	34.0
3	Four-ply, medium weight, unbalanced weave, nylon fabric, Buna-N coated.	950	168,600	32.0
4	Three-ply, heavy weight, plain weave, nylon fabric, Buna-N coated	1,200	201,800	30.5
5	Four-ply, unidirection, medium weight, nylon-cord fabric, nonintegral lightweight bladder-cell liner for diffusion barrier	950	171,000	30.0

*Tensile strength, energy absorption, and elongation as determined with the compressed-air gun. These values are not comparable to those obtained by standard fabric-test procedures.

---

[4] Motsinger, Miller, and Schroers, op. cit.

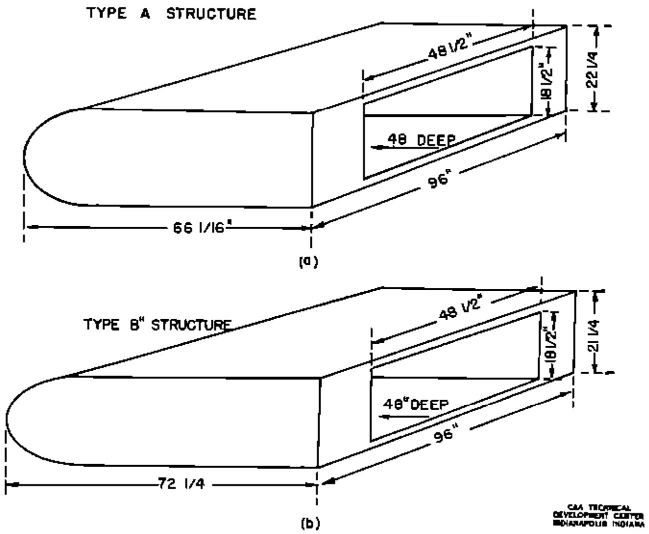

Fig. 2 General Dimensions of Types A and B Structures

The supply of bladder cells and wing structures was broken down further so as to provide 10 different configurations of test specimens with 5 specimens of each configuration for test purposes. A test specimen is defined as a simulated wing structure equipped with a bladder cell.

The spanwise variation of ultimate allowable chordwise shear and bending moment for the wings of the two-engine and four-engine aircraft used in the tests is shown in Figs. 4 and 5 respectively. The chordwise bending moment and shear strength of the Types A and B structures are represented by the crosshatched areas of these figures.

All tests were conducted with the bladder cell 97 per cent full of water. The Type A structure, fuel cell, and its fluid weighed approximately 1800 pounds. The Type B unit and its contents weighed approximately 2000 pounds.

A photograph of the impact-test facility is shown in Fig. 6. The experimental fuel cell and simulated wing structures were mounted on a car which operated on a track 300 feet in length. This car was propelled by a Navy Mark IV catapult to velocities as high as approximately 100 mph. A system of arresting cables near the track terminal stopped the car, permitting the test unit to be propelled into the sandbag-faced backstop.

Two movie cameras operating at approximately 1500 frames per second were used to obtain a time history of the impact. A fluid-pressure-sensing device was used to record the internal fluid pressure. The signals from the pressure-sensing unit were transmitted through a trailing cable to a recording oscillograph.

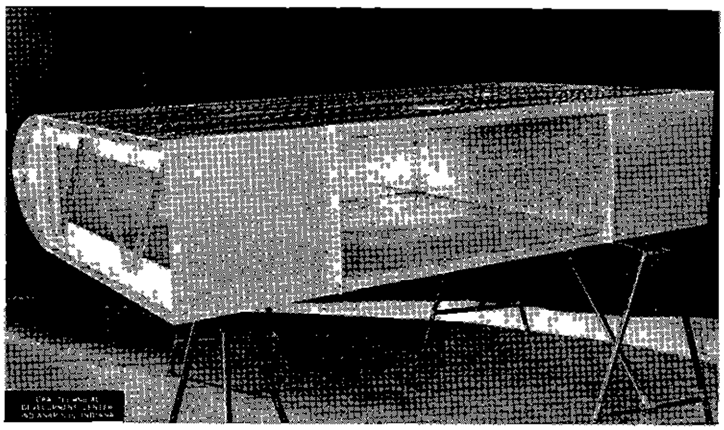

Fig. 3 Type B Structure

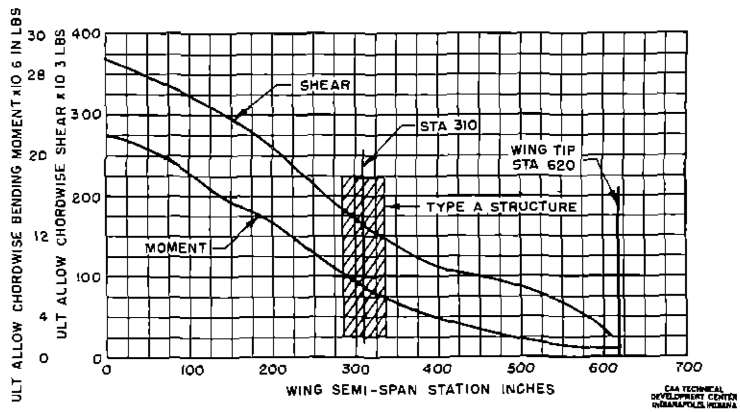

Fig 4 Ultimate Allowable Chordwise Shear and Bending Moment Versus Span of Wing of Twin-Engine Airplane

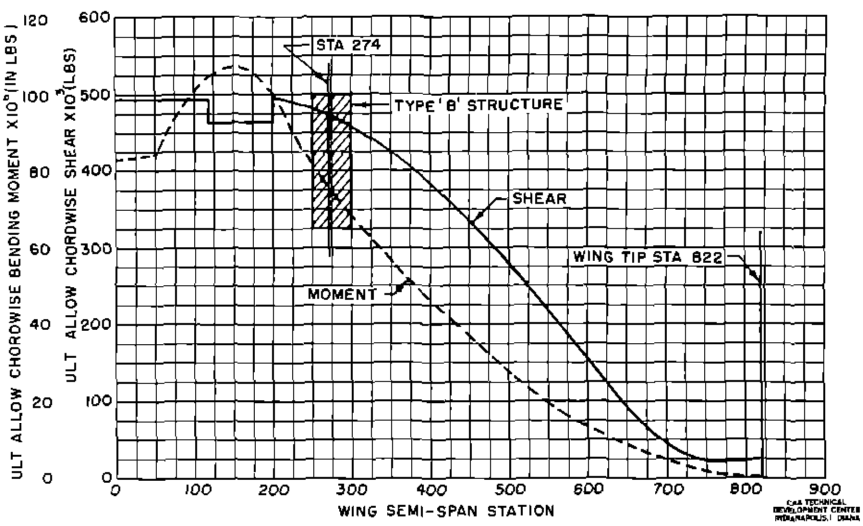

Fig 5 Ultimate Allowable Chordwise Shear and Bending Moment Versus Span of Wing of Four-Engine Airplane

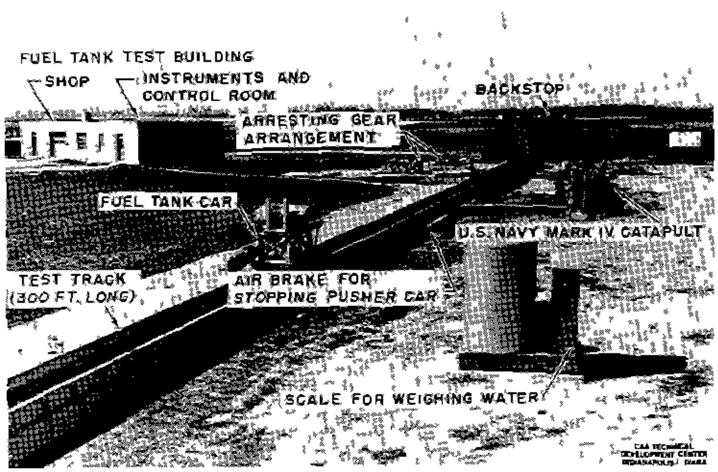

Fig 6 View of Facilities for Conducting Crash Tests on Aircraft Fuel Tanks

TEST PROCEDURE

The maximum tensile strength and energy-absorbing properties of the five bladder-cell materials were obtained from burst tests on the compressed-air gun under ambient climatic conditions and without exposure to aircraft fuels The load-versus-elongation curve for each specimen of a material was obtained by plotting the load against the percentage of material elongation These factors were obtained from information provided by pressure transducers and high-speed movie records The maximum tensile strength was taken directly from such curves A number of these curves then were used to determine a mean load-versus-elongation curve for each material The mean load-versus-elongation curves were used to construct a mean pressure-versus-volume diagram for each type of material The area under the pressure-versus-volume diagram was integrated graphically, and the area thus found represents the energy-absorbing ability of a piece of the material 34 1/2 inches in diameter The reasons for selecting a specimen of this particular size are discussed in a previous report [5]

Five test specimens were available to establish the impact resistance of a particular metal-structure bladder-cell configuration An attempt was made in the first two tests to establish its general range of ultimate impact resistance Succeeding tests then were conducted to define more accurately the maximum impact resistance

The time history of the tank position during impact was obtained directly from high-speed movie records The rate of change of these data resulted in a time history of the velocity during impact The time history of the deceleration then was obtained by determining the rate of change in velocity The area under the deceleration-versus-time curve was integrated graphically and was divided by total impact time to yield the average deceleration experienced by the cell and structure during impact All deceleration data presented were measured at a point approximately six inches aft of the front spar

All deceleration data are presented in terms of load factor by dividing deceleration (feet per second per second) by the gravitational constant (32 2 feet per second per second) The impact load may be obtained from the equation

$$\text{Impact Load} = W \times n \qquad (1)$$

where

W = weight of the metal structure, bladder cell, and fluid contents, in pounds

n = load factor

A fuel tank undergoing a typical impact test is shown in Fig 7 A Type A structure and a Type B structure which have been subjected to impact tests are shown in Figs 8 and 9, respectively A bladder cell is shown in Fig 10

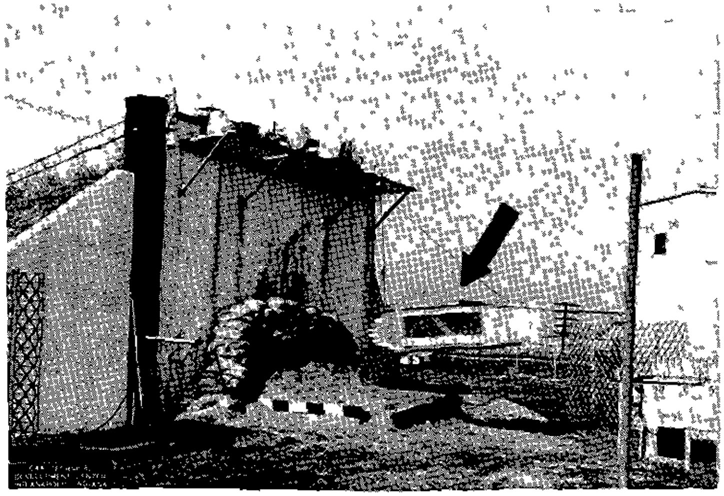

Fig 7 Fuel Tank Undergoing an Impact Test

[5] Motsinger, Miller, and Schroers, op cit

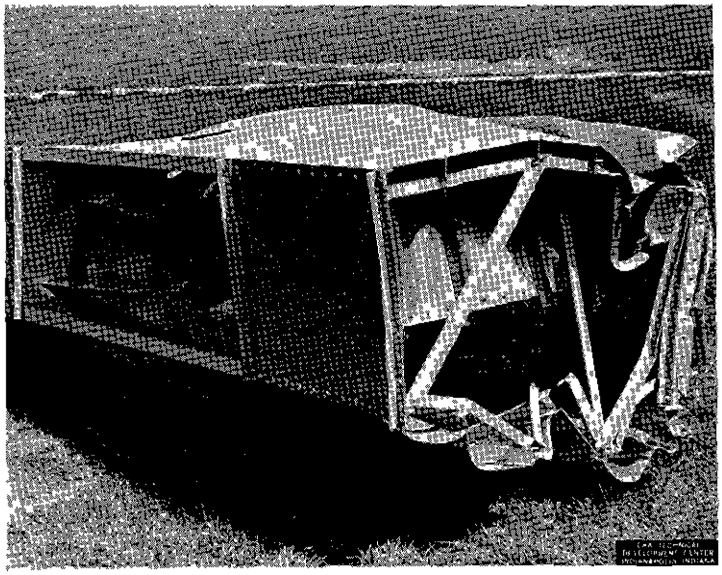

Fig 8 A Type A Structure Which Has Been Subjected to an Impact Test

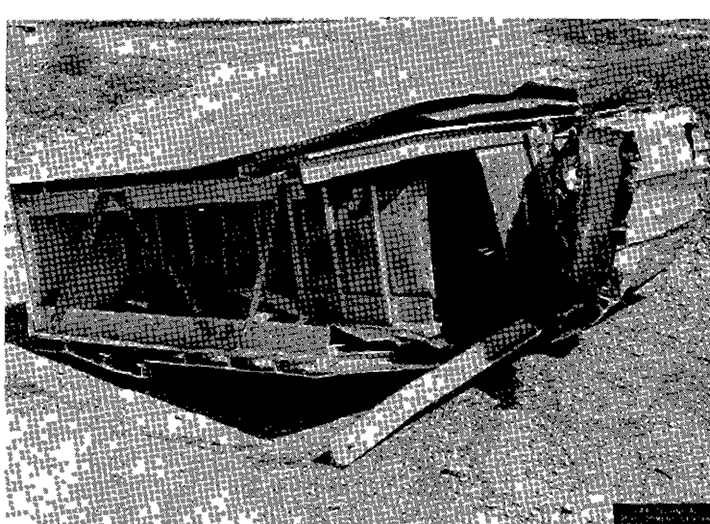

Fig 9 A Type B Structure Which Has Been Subjected to an Impact Test

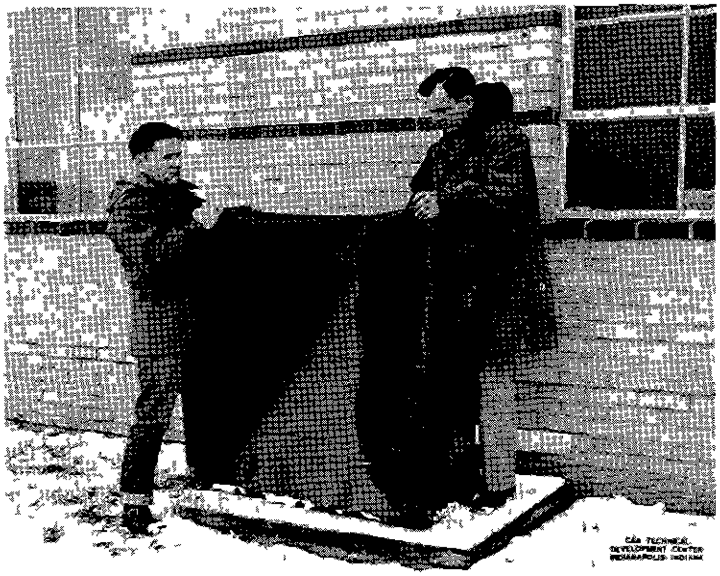

Fig 10 Typical Bladder Cell Prior to Test

RESULTS AND DISCUSSION

The mean load-versus-elongation curves and the pressure-versus-volume diagrams for the five groups of materials used in the tests are shown in Figs 11 and 12, respectively The ultimate tensile strength and the energy-absorbing properties of these materials, as determined with the compressed-air gun, also are given in Table I

The results of all impact tests are summarized in Table II In 8 of the 50 tests conducted, either satisfactory data were not obtained or the test was judged to be invalid for some reason Consequently, the results of 42 rather than of 50 tests are shown in the table

The time histories of the deceleration, in terms of load factor for the impact tests conducted, are shown in Figs 13 and 14 for the Types A and B structures, respectively

As previously described, the average deceleration experienced by each test unit during impact was obtained by measuring the area under the deceleration-versus-time curve and dividing it by total impact time The internal fluid pressures measured by a pressure-sensing device located approximately 6 inches behind the forward wall of the tank are given in Table II These pressures, based on the 3 1/2-foot head of water, were determined to be equivalent to those which would result from decelerations approximately equal to the average decelerations Therefore, it is apparent that the peak impact decelerations experienced by the simulated wing structures were not transmitted to the confined fluid

The inability in some cases to establish from the photographic records the absolute peak deceleration experienced by the simulated wing structure made it necessary to determine a general relationship between the average impact deceleration and the peak deceleration An analysis of the impact-test results indicates that the well defined peak decelerations were in the order of 3 5 times the average decelerations In general, therefore, the peak decelerations have been considered as being 3 5 times the average

The results of the impact tests are shown in Figs 15 and 16 Figure 15 shows the relationship between tensile strength of the fuel-cell material as determined with the compressed-air gun, fluid pressure in the fuel cell, and peak impact load on the structure for two different wing structures Figure 16 is the same as Fig 15 except that energy-absorbing properties of the fuel cell as determined with the compressed-air gun are plotted in place of tensile strength of the fuel cell

To obtain these curves, the average decelerations listed in Column 4, Table II, first were plotted against the fuel-cell tensile strength and energy-absorbing properties given in Table I The slope of the curves and their positions with respect to each other were established from such plotted points The parameter, peak impact load, or simply the impact load, plotted along the abscissa in Figs 15 and 16, then was obtained by multiplying the average decelerations by the factor 3 5 and by the total weight of the test unit, in pounds In

TABLE II

IMPACT-TEST RESULTS

Test No	Wing Structure (type)	Fuel Cell Material No	Average Deceleration (n)*	Approximate Maximum Peak Deceleration** (n)*	Bladder-Cell Failure	Recorded Fluid Pressure (pounds per square inch)	Duration of Impact (seconds)	Deceleration Calculated from Measured Pressure (n)*
1	A	1	15 0	52 5	No	17 4	0 060	11 5
2	A	1	14 9	52 2	Yes	24 65	0 065	16 3
3	A	1	13 5	47 3	No	17 55	0 070	11 6
4	A	2	18 3	64 0	Yes	--	0 100	--
5	A	2	10 4	36 4	No	--	0 085	--
6	A	2	26 5	92 7	Yes	52 13	0 070	33 0
7	A	2	29 9	104 7	Yes	64 36	0 080	42 4
8	A	3	26 5	92 7	Yes	35 78	0 070	23 6
9	A	3	25 8	90 4	Yes***	42 87	0 068	28 2
10	A	3	14 9	52 2	No	37 86	0 084	24 9
11	A	3	21 5	75 3	No	40 34	0 084	26 6
12	A	4	31 0	108 4	No	--	0 085	--
13	A	4	23 2	81 3	Yes	--	0 090	--
14	A	4	22 0	77 0	No	--	0 080	--
15	A	5	53 0	185 5	Yes	71 5	0 055	47 0
16	A	5	26 0	91 0	No	--	0 060	--
17	A	5	46 0	161 0	Yes	71 94	0 060	46 4
18	A	5	48 5	170 0	No	59 13	0 065	39 0
19	A	5	50 0	175 0	No	64 73	0 045	33 0
20	B	1	51 8	181 5	Yes	123 16	0 030	81 2
21	B	1	45 05	152 8	Yes	--	0 045	--
22	B	1	18 70	65 5	No	47 73	0 065	31 4
23	B	1	24 10	84 4	No	42 29	0 060	27 8
24	B	2	42 5	148 8	No	63 64	0 050	42 0
25	B	2	40 9	143 0	No	61 09	0 050	40 3
26	B	2	67 5	236 0	No	93 56	0 040	61 6
27	B	2	49 8	174 0	No	105 14	0 050	69 6
28	B	2	69 2	242 0	Yes	152 66	0 040	100 5
29	B	3	46 2	161 8	Yes	52 53	0 052	34 6
30	B	3	40 4	141 3	No	72 31	0 050	46 7
31	B	3	36 8	128 9	Yes	55 63	0 050	36 7
32	B	3	34 6	121 0	No	60 52	0 060	39 8
33	B	4	35 6	124 6	No	--	0 065	--
34	B	4	42 8	149 8	No	--	0 050	--
35	B	4	70 4	246 4	Yes	148 8	0 040	97 8
36	B	4	33 6	117 6	No	107 05	0 060	70 7
37	B	4	53 6	187 6	Yes	103 71	0 050	68 3
38	B	5	47 5	166 1	No	88 83	0 045	58 5
39	B	5	89 5	131 3	Yes	106 58	0 035	70 4
40	B	5	116 2	407 0	No	125 71	0 030	82 9
41	B	5	85 2	298 0	Yes	140 83	0 036	92 8
42	B	5	55 5	194 1	No	81 62	0 040	53 8

*Load factor
**Approximate maximum peak deceleration is taken as 3 5 times value in Column 4
***Slight break

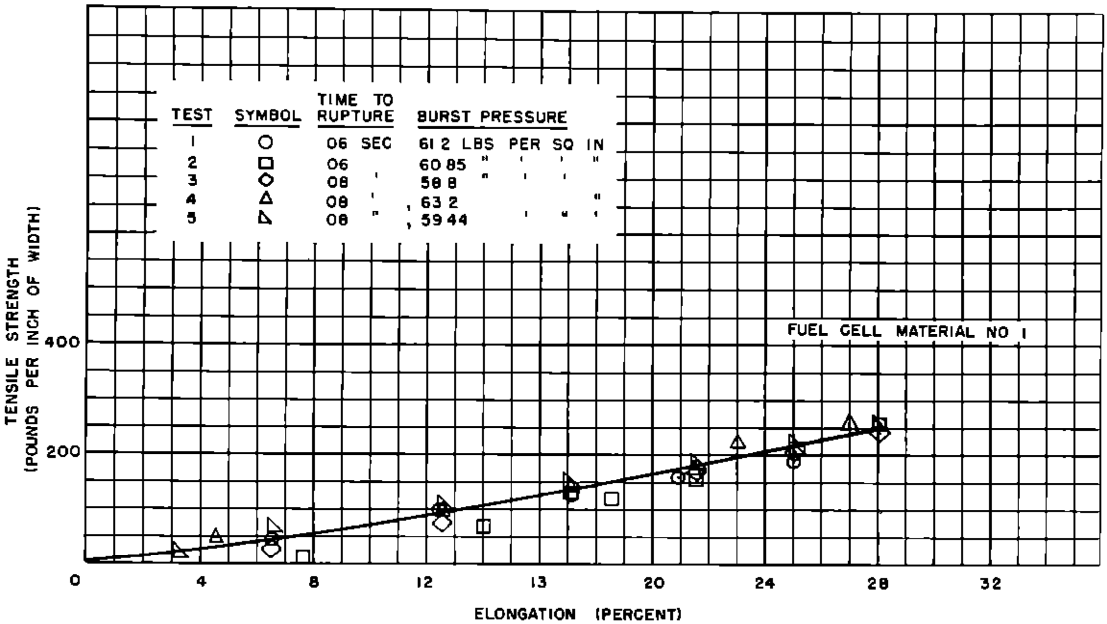

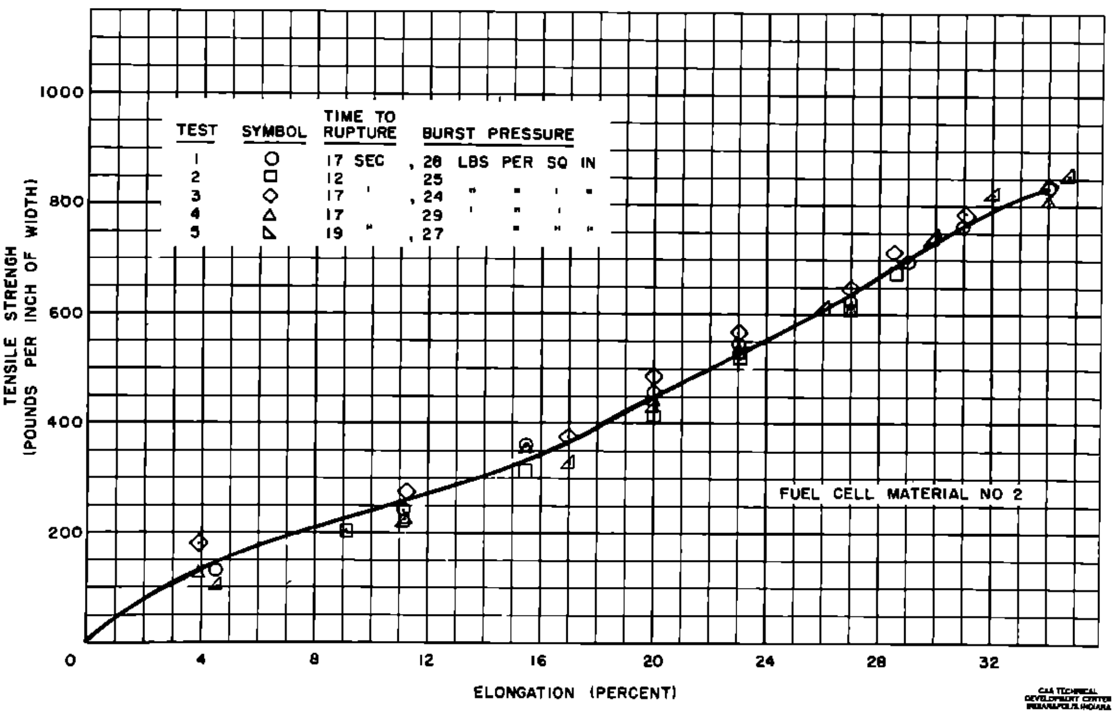

Fig 11 Load-Elongation Curves of Bladder-Cell Test Materials

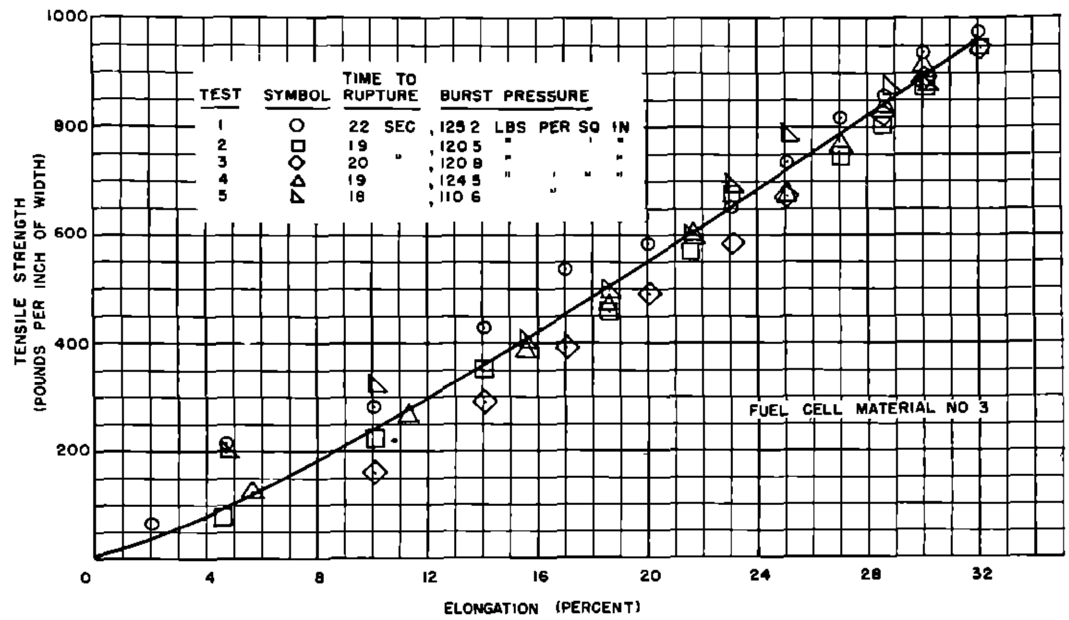

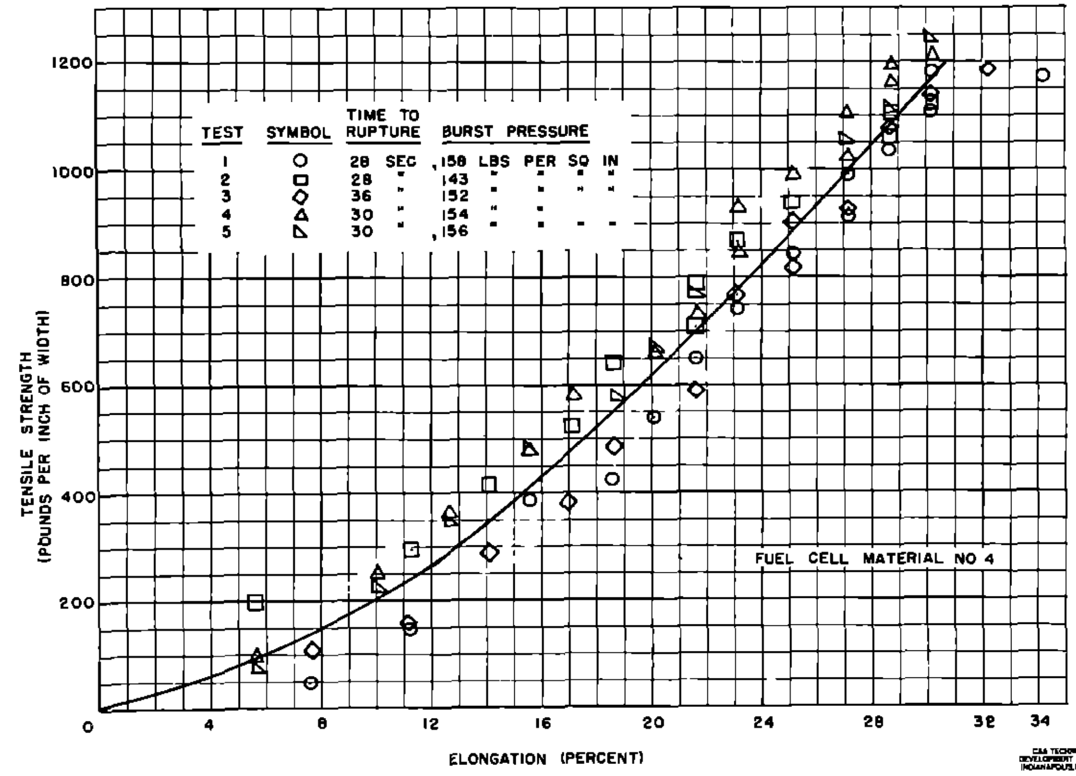

Fig 11 Load-Elongation Curves of Bladder-Cell Test Materials (Continued)

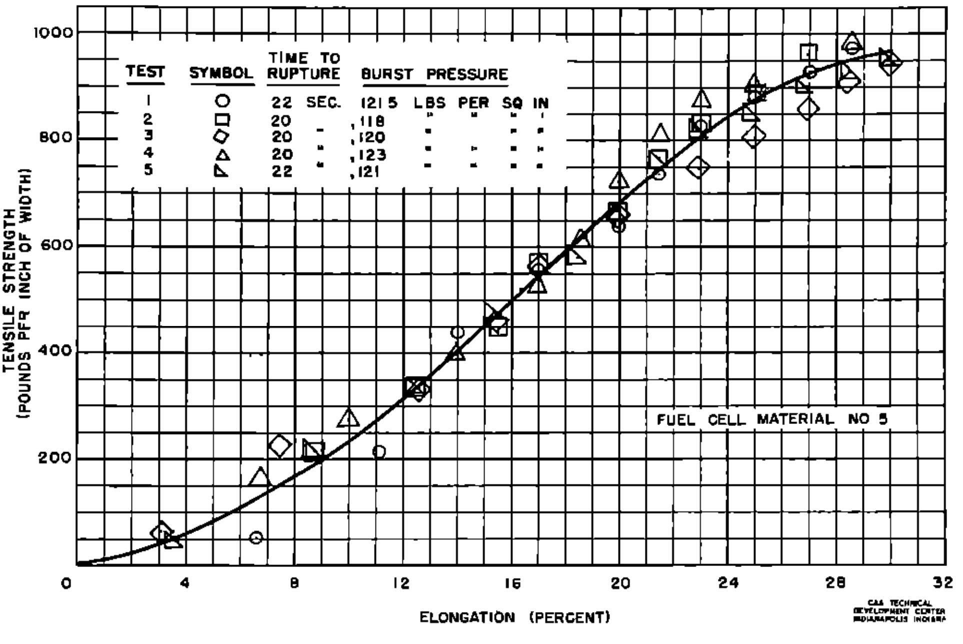

Fig 11 Load-Elongation Curves of Bladder-Cell Test Materials (Continued)

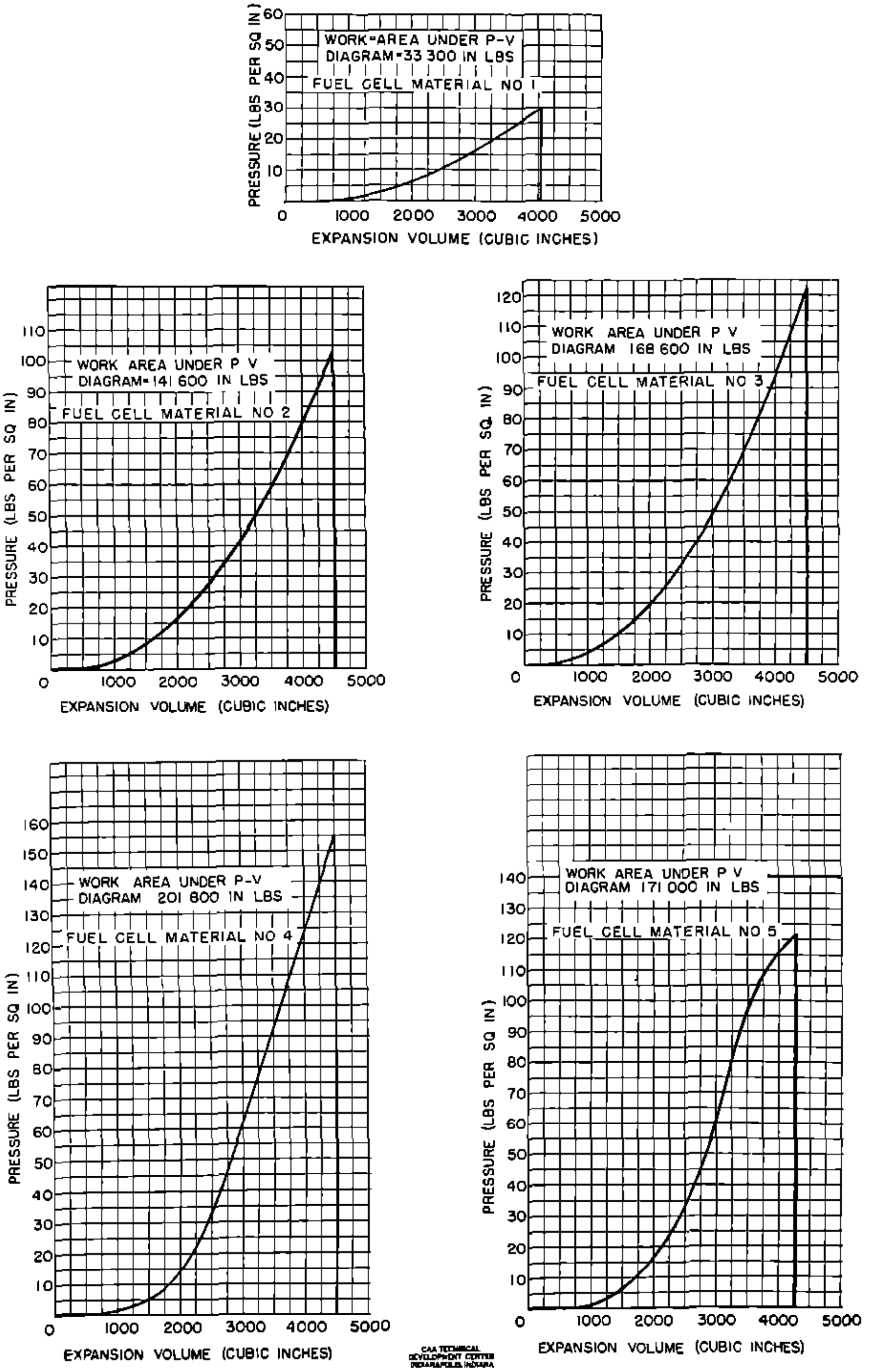

Fig 12 Pressure-Volume Diagrams of Bladder-Cell Test Materials

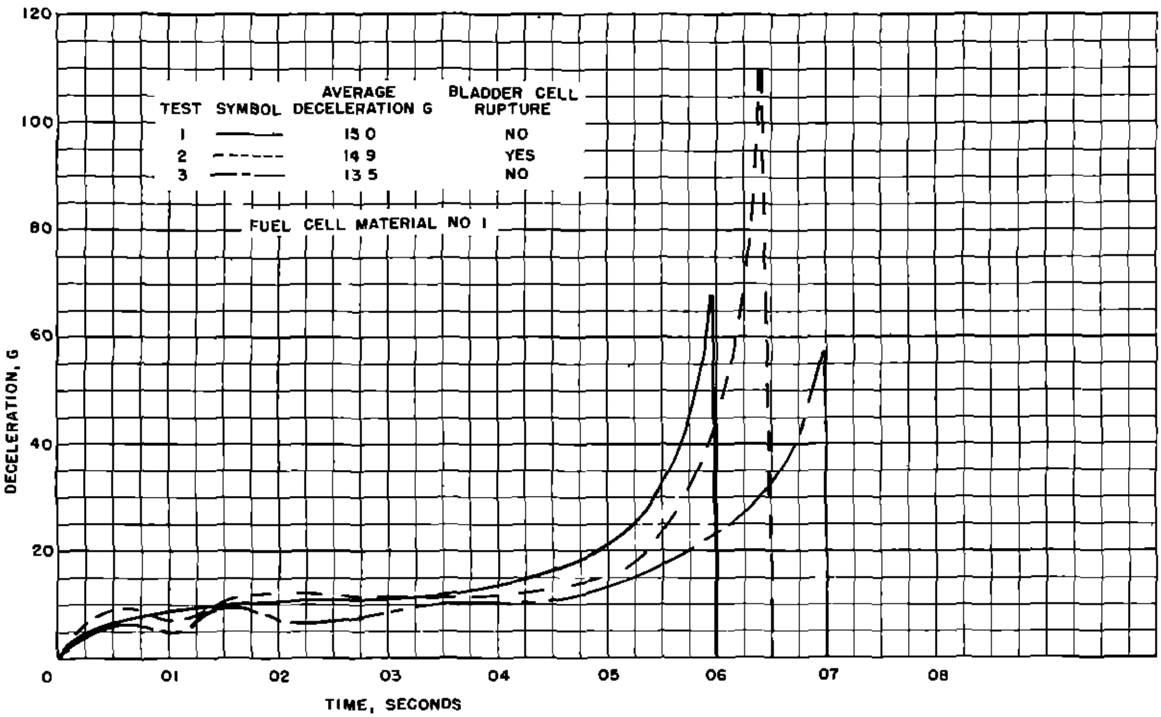

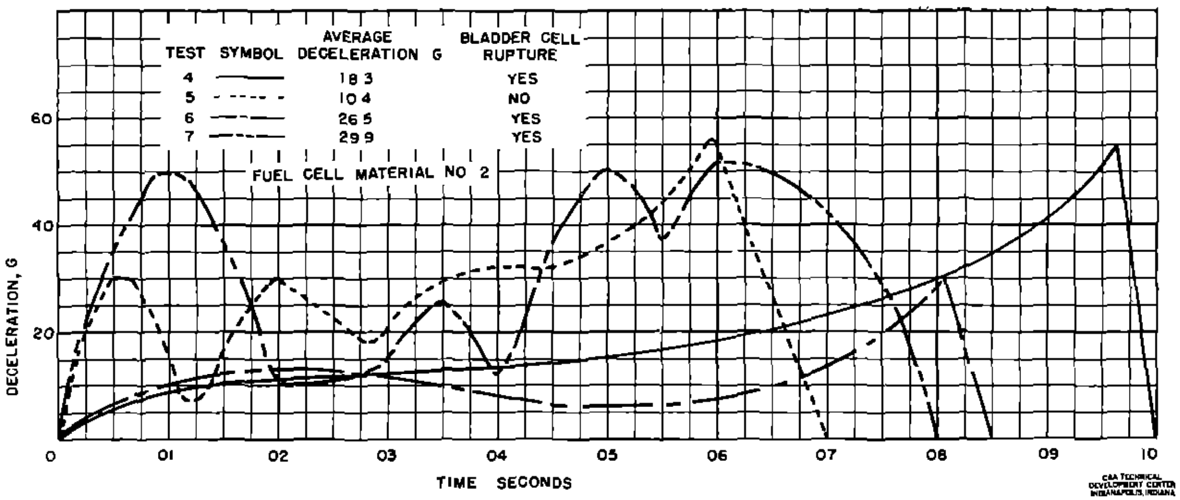

Fig 13 Time History of Impact Deceleration of Type A Structure

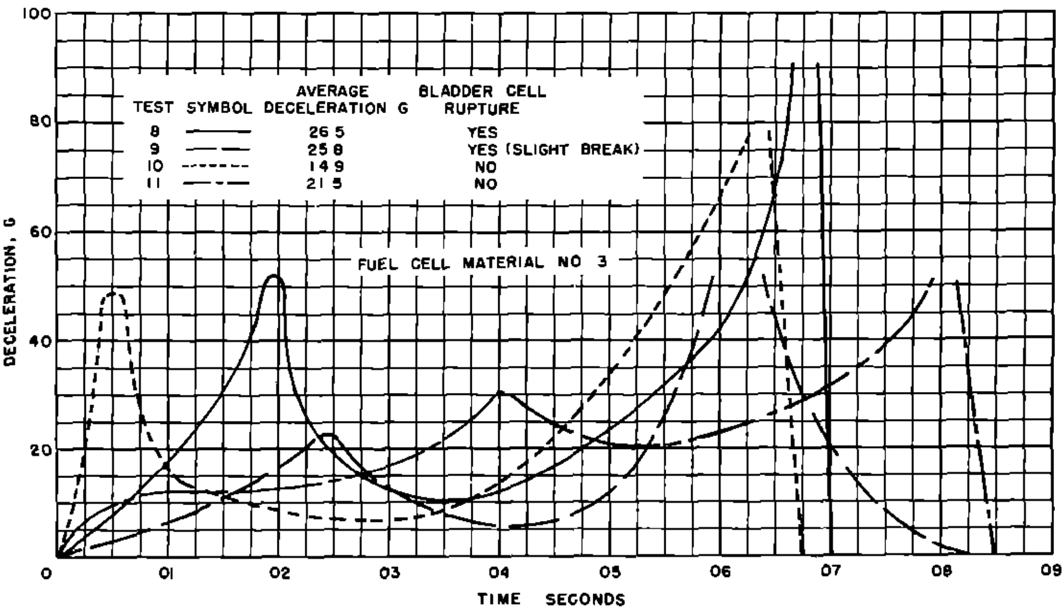

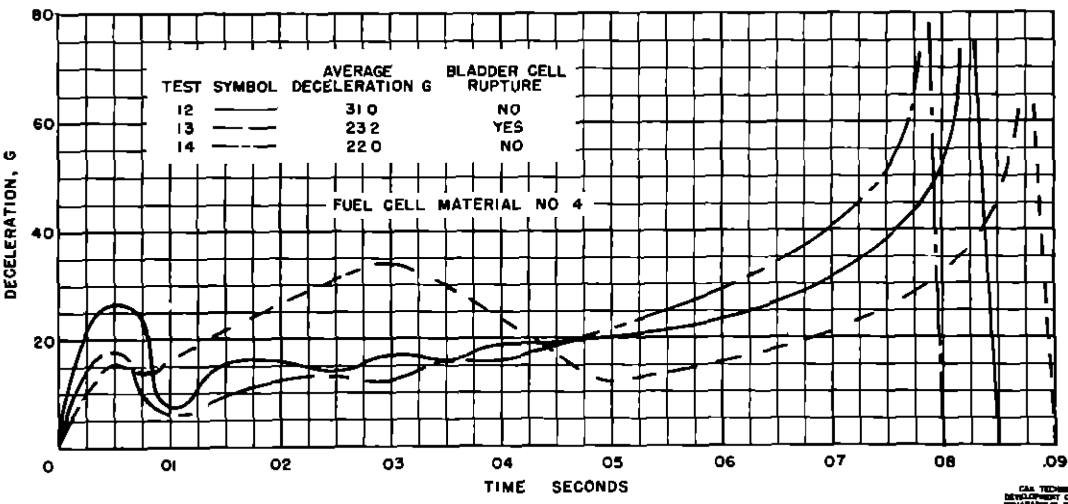

CAA TECHNICAL DEVELOPMENT CENTER INDIANAPOLIS INDIANA

Fig 13 Time History of Impact Deceleration of Type A Structure (Continued)

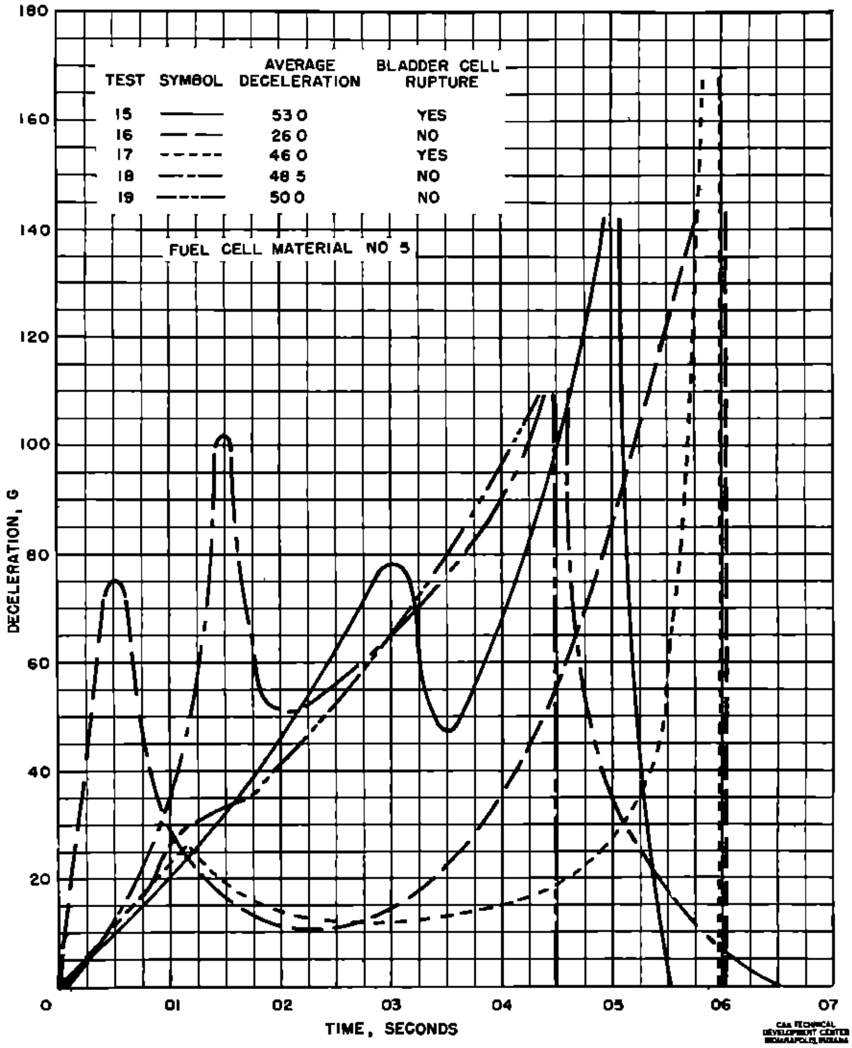

Fig 13 Time History of Impact Deceleration of Type A Structure (Continued)

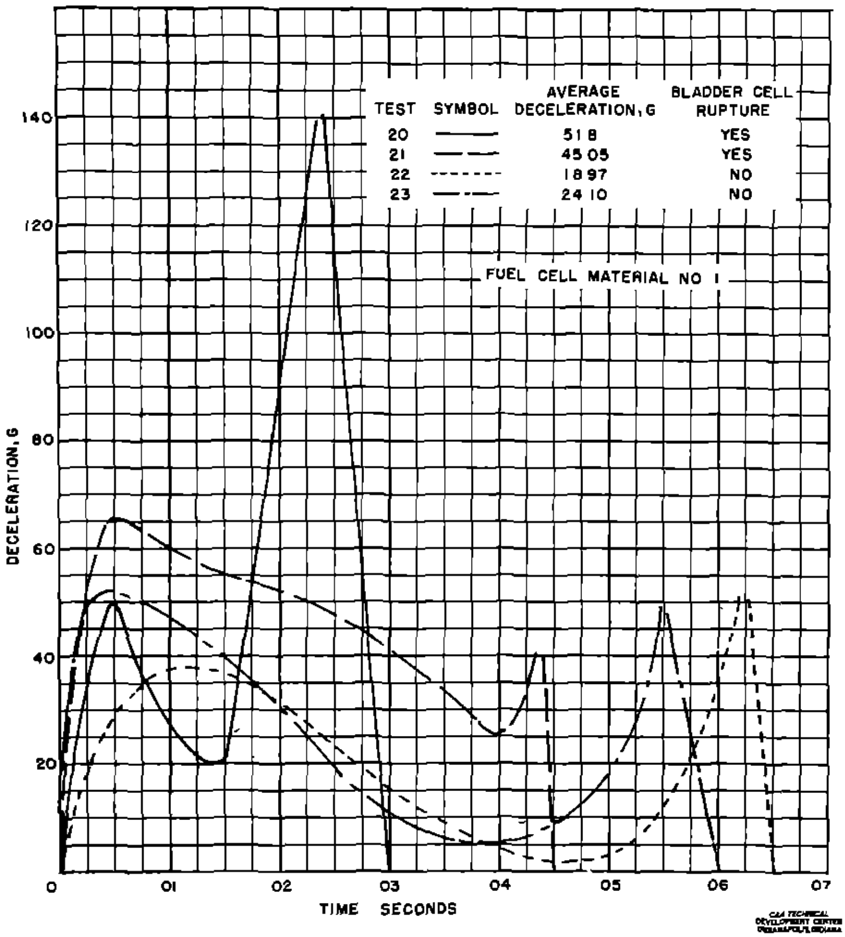

Fig 14 Time History of Impact Deceleration of Type B Structure

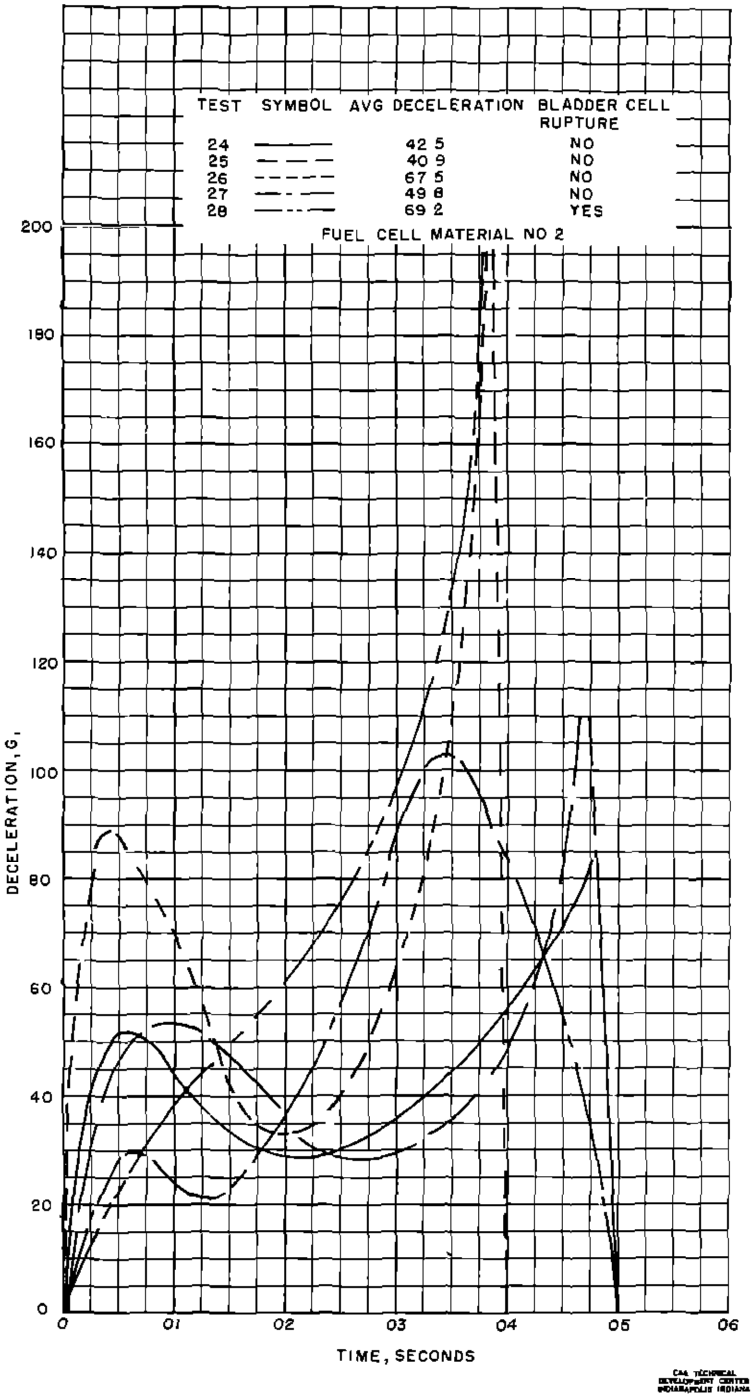

Fig. 14 Time History of Impact Deceleration of Type B Structure (Continued)

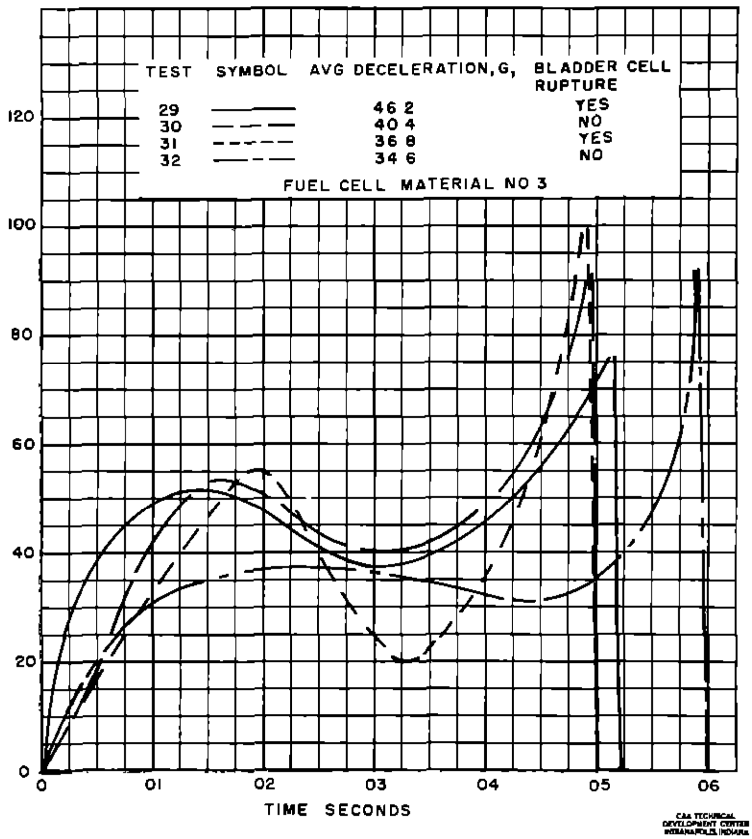

Fig 14 Time History of Impact Deceleration of Type B Structure (Continued)

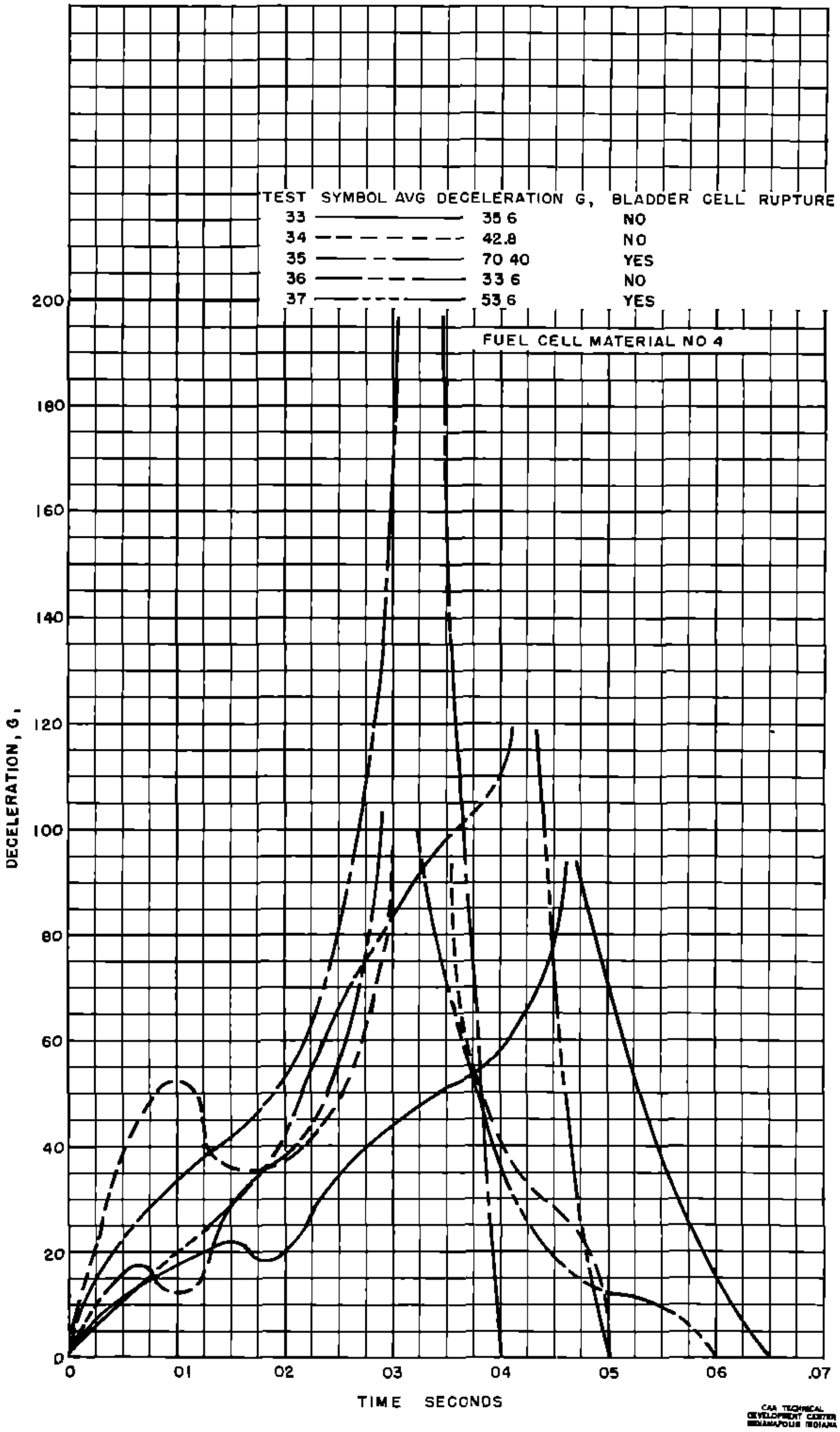

Fig 14 Time History of Impact Deceleration of Type B Structure (Continued)

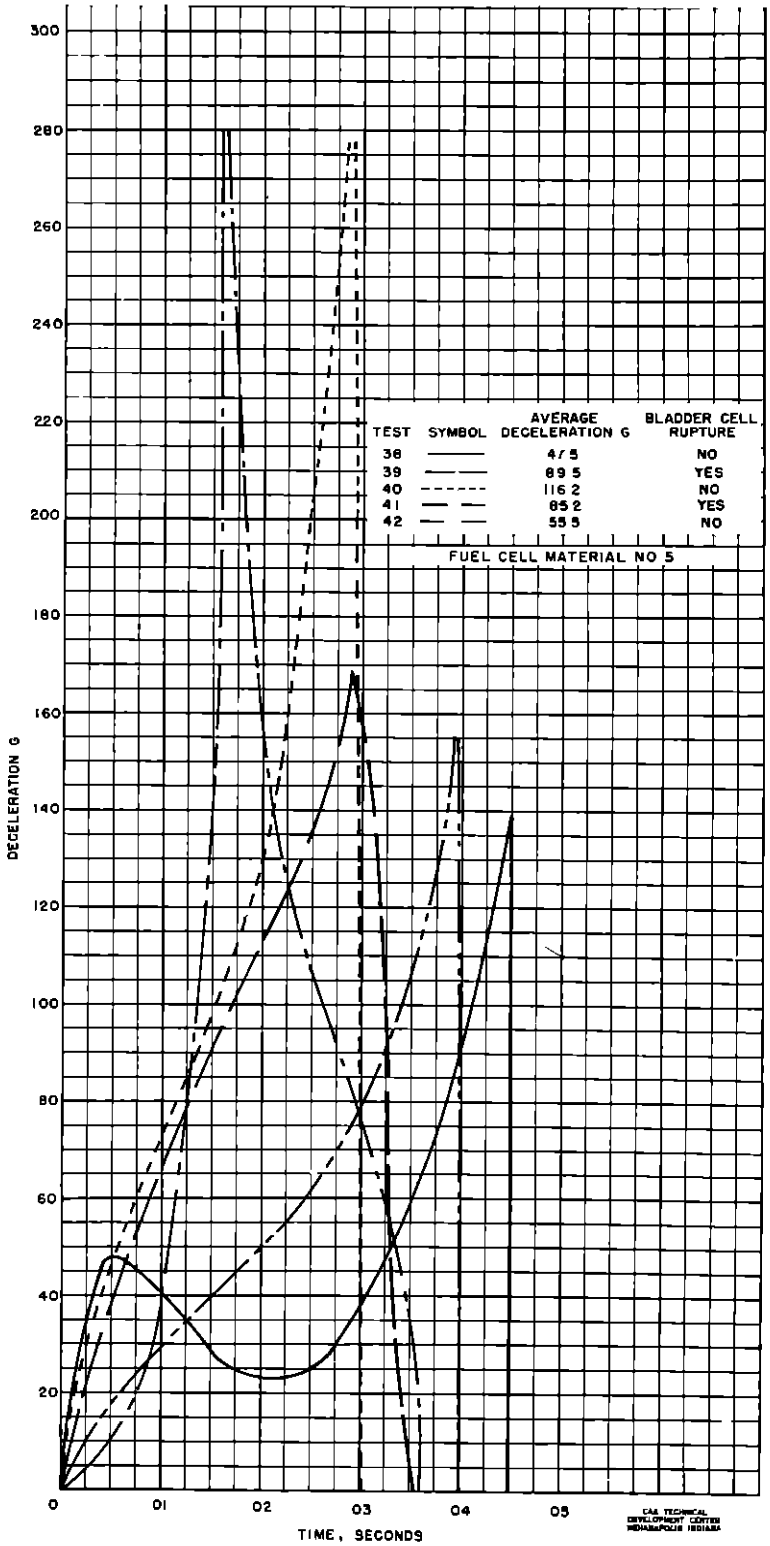

Fig 14 Time History of Impact Deceleration of Type B Structure (Continued)

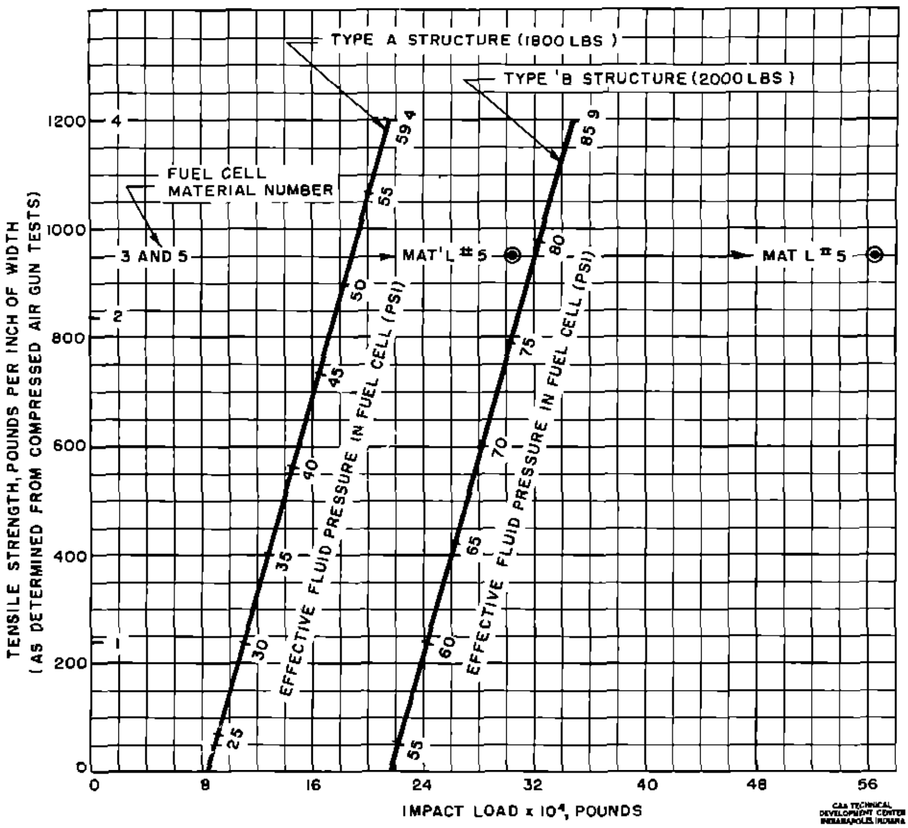

Fig 15 Correlation of Required Bladder-Cell Tensile Strength and Fluid Pressures with Impact Load

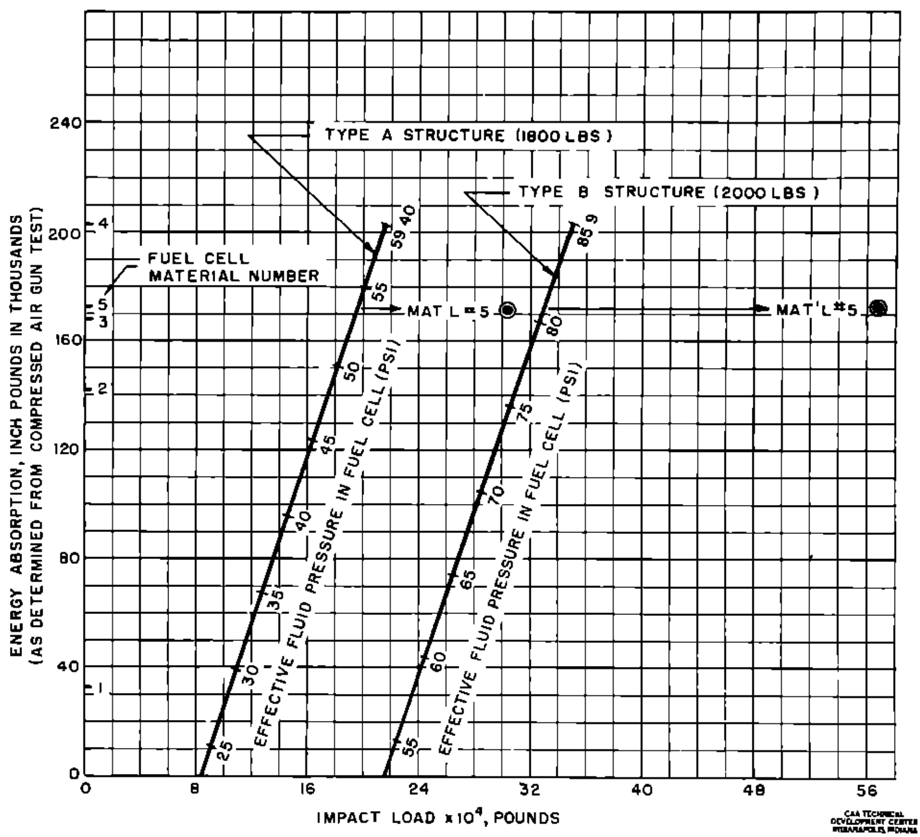

Fig. 16 Correlation of Required Bladder-Cell Energy-Absorption Properties and Fluid Pressures with Impact Load

establishing the curves, it should be realized that appreciable load is not applied to the bladder-cell material until substantial failure occurs in the inner structural compartment supporting the bladder cell From impact-test experience it is known also that the degree and the manner of structural failure are not always consistent with magnitude of impact load In some cases, therefore, failure of the cell did not define exactly the ultimate impact resistance of the structure-bladder-cell combination. In addition, with the five test units available, it was not always possible to narrow the range of impact load sufficiently to define closely the allowable impact resistance of a test unit This was particularly true for material No 1 in the Type B structure The impact resistance of this combination was determined by extrapolation of data on materials Nos 2, 3, and 4 in the Type B structure From Columns 4 and 9, Table II, it also can be seen that decelerations calculated from measured maximum fluid pressures in the fuel cells compared quite favorably with the average decelerations obtained from the high-speed movie records Therefore, the maximum pressure appears to be associated with the average deceleration rather than with the peak deceleration Fluid pressures corresponding to a water head of four feet and mean deceleration of the metal structure, therefore, have been superimposed on the curves

These data indicate that the allowable impact load on the simulated wing structure without experiencing fuel-cell rupture, using fuel-cell materials Nos 1, 2, 3, and 4, varies linearly with the tensile strength and energy-absorbing properties of the fuel-cell material Because of the linear variation of material tensile strength and energy-absorbing properties with impact resistance, the impact-test data have been extended to a theoretical point of zero bladder-cell strength The two points of zero bladder-cell strength were verified in the tests by the fact that impact loads of less than approximately 80,000 pounds for the Type A structure and of less than approximately 220,000 pounds for the Type B structure did not result in failure of the portion of the structure supporting the bladder cell Until the supporting structure fails, no appreciable load is applied to the bladder

A comparison of the impact-test data for the two structures indicates that the increased structural strength of the Type B structure provides increased crash resistance equivalent to approximately 140,000 pounds This effect is attributed primarily to the greater leading-edge strength of the Type B structure, however, the over-all strength of the Type B structure is recognized to be an important contributing factor

The effect of cell construction may be noted by comparing the impact-test results of materials Nos 3 and 5 Although these materials exhibited approximately equal strength, elongation, and energy-absorbing properties in the compressed-air gun tests, the impact resistance of the cells was considerably different Cells constructed of material No 5 exhibited an ability to withstand greater impact loads The cells constructed from material No 5 contained a nonintegral, lightweight bladder-cell liner for a diffusion barrier, and they also were reinforced by the addition of extra plies of fabric at vulnerable locations determined by previous tests These differences in cell construction, along with the difference in basic material (No 5, tire cord, No 3, woven fabric), are considered responsible for the impact-resistance variation

Certain adjustments and corrections must be applied to the data in Figs 15 and 16 in order to determine the strength and energy-absorbing properties of fuel cells for actual aircraft Data on these corrections are being obtained through impact tests on two aircraft models having wing stiffness and properly proportioned and distributed mass characteristics equivalent to those of the modern twin-engine and four-engine transport airplanes mentioned previously The results of the tests on the wing models will be presented in a subsequent report Information derived from the model tests, applied in conjunction with the data in Figs 15 and 16 to an actual aircraft, will permit calculation of the strength and energy-absorbing properties of crash-resistant fuel cells for that aircraft in accordance with the concepts on fuel-tank design criteria described in this report

Because water rather than fuel was used in the impact tests, calculations on strength and energy-absorbing properties of fuel cells for actual aircraft may take into account the beneficial effect of the lower density of fuel compared to that of water This also will be covered in a subsequent report

CONCLUSIONS

The results of tests conducted to correlate the ability of a nonmetallic-type fuel tank, when installed in a simulated wing structure to resist rupture under impact loads with material strength and/or energy-absorbing properties, can be summarized as follows

1 Impact resistance varied linearly with the strength and energy-absorbing properties of the material for materials of similar construction

2 Impact resistance is affected greatly by fuel-cell construction

3 Impact resistance can be increased by increasing the strength of the surrounding structure